Identification of S_2O_4 in sulfur dioxide solutions in HMPA

Elisabeth Potteau, Eric Levillain and Jean-Pierre Lelieur*

Laboratoire de Spectrochimie Infrarouge et Raman (LASIR, CNRS UPR 2631), Hautes Etudes Industrielles (HEI), 13, Rue de Toul, 59046 Lille cedex, France

Received (in Montpellier, France) 14th May 1998, Accepted 20th July 1998

The characteristics of the UV/VIS absorption spectra of SO_2 solutions in HMPA have been accurately determined. The decomposition of the spectra by a nonlinear least-squares method shows the existence of two bands. The analysis of the absorbance variations of each band *versus* the total SO_2 concentration shows that SO_2 is in equilibrium with the dimer species S_2O_4. Quantitative analysis of these variations allows us to determine the equilibrium constant of the dissociation of S_2O_4 (into two SO_2 units): $K = (1.3 \pm 0.4) \times 10^{-2}$ mol dm^{-3}. The influence of the addition of a supporting electrolyte has been examined: it shifts the equilibrium towards SO_2, as expected for equilibria involving neutral species. The existence of S_2O_4 is also supported by the Raman spectra of SO_2–HMPA solutions.

These results have been correlated with an electrochemical study; the S_2O_4 reduction is observed as a prewave in the cyclic voltammograms at a potential about 150 mV higher than that of the reduction of SO_2. This is also indicated by the difference of the electron affinity of these two species, which have been computed here. Moreover, the intensity of the prewave is related to the concentration of S_2O_4 in the solution. This confirms both the existence of this species and the attribution of the prewave to its reduction.

Identification de S_2O_4 dans les solutions de dioxyde de soufre dans HMPA. Les caractéristiques des spectres d'absorption UV/VIS des solutions de SO_2 dans HMPA ont été déterminées avec précision. La décomposition des spectres par une méthode de moindres carrés non linéaires indique l'existence de deux bandes d'absorption. L'étude des variations d'absorbance de chaque bande avec la concentration totale en SO_2 montre que SO_2 est en équilibre avec une espèce dimère S_2O_4. L'analyse quantitative de ces variations permet de déterminer la constante d'équilibre de la dissociation de S_2O_4 (en 2 SO_2): $K = (1.3 \pm 0.4) \times 10^{-2}$ mol dm^{-3}. L'influence de l'ajout d'un électrolyte support a été examinée: l'équilibre se déplace vers SO_2, comme prévu pour les équilibres faisant intervenir des espèces neutres. L'existence de S_2O_4 a également été mise en évidence par spectroscopie Raman des solutions SO_2–HMPA.

Ces résultats ont été corrélés avec l'étude électrochimique: la réduction de S_2O_4 est observée sous la forme d'une prévague sur les voltammogrammes, à un potentiel supérieur d'environ 150 mV par rapport à la réduction de SO_2. Le calcul de l'affinité électronique de ces deux espèces indique également une réduction légèrement plus facile pour S_2O_4. De plus, l'intensité de la prévague est liée à la concentration de S_2O_4 dans la solution. Ceci confirme à la fois l'existence de cette espèce et l'attribution de la prévague à sa réduction.

The study of the reduction of sulfur dioxide in nonaqueous solvents led us to determine a way of stabilizing the reduced species of sulfur dioxide. We have recently shown[1] that these species, resulting from the chemical reduction of sulfur dioxide by lithium, can be stabilized in hexamethylphosphoramide (HMPA). The polythionite solutions $Li(SO_2)_n$–HMPA, obtained by this method, have been investigated by ESR and UV/VIS absorption spectroscopy.[1] In the spectrophotometric study, a quantitative analysis of the absorption spectra is currently in progress; for this purpose, it is necessary to know the value of the molar extinction coefficient of sulfur dioxide in HMPA. To our knowledge, this value is not reported in the literature. The spectrophotometric study of SO_2–HMPA solutions was performed in order to determine the spectrophotometric characteristics of SO_2.

This study gave evidence of a dimerization equilibrium of SO_2 in HMPA, as will be reported in the present paper. The existence of a sulfur dioxide dimer S_2O_4 in solution has only been proposed once: Devèze and Rumpf[2] investigated by spectrophotometry SO_2 solutions in nonpolar solvents. They observed a deviation from Beer–Lambert's law, which they interpreted as the autoassociation of SO_2 into a dimer species, but no spectroscopic characterization of this species was given. However, S_2O_4 has been observed in gaseous SO_2,[3] in liquid SO_2 [4] and in SO_2 trapped in argon matrices at 20 K.[5] Moreover, the cyclic voltammetric study of polythionite solutions[6] suggested the existence of S_2O_4 in SO_2–HMPA solutions. Another aim of the present work was then to identify the S_2O_4 species in SO_2–HMPA solutions.

Several authors studied SO_2 solutions in nonaqueous solvents, because SO_2 is known to form charge–transfer complexes with Lewis bases.[7–10] These complexes are characterized by a UV/VIS absorption band at about 290 nm. The most widely studied complexes result from the interaction of SO_2 with amines,[7,8] but SO_2 can also form complexes with aromatic compounds, olefins and oxygenated compounds.[9,10]

We present in this paper a detailed spectrophotometric study of sulfur dioxide solutions in HMPA. These results are correlated with Raman spectra and with the prewave observed in cyclic voltammetric experiments performed on the same solutions. These techniques give evidence of the dimerization of SO_2 in HMPA.

Experimental

Materials

The reasons for choosing hexamethylphosphoramide (HMPA) as a solvent have been given elsewhere.[6] HMPA (Aldrich, 99%) is dried on NaH for at least 24 h, then distilled twice at

100 °C.[11] SO_2 (L'Air Liquide, >99.7%) is purified on H_2SO_4 then on P_2O_5.[4] Tetraethylammonium perchlorate (TEAP, Fluka, >99%) is dried *in vacuo* at 150 °C for at least 24 h. It is used as a supporting electrolyte at a concentration of 0.1 mol dm^{-3}.

Apparatus

UV/VIS absorption spectra have been recorded using a Perkin–Elmer Lambda 19 UV/VIS/NIR spectrophotometer. The spectra have been recorded at room temperature between 230 (solvent cut-off) and 600 nm. The large concentration range investigated implied the use of optical cells with different pathlengths, between 0.1 and 5 mm. In order to simplify the presentation of the data, the absorbance value has been divided by the optical pathlength expressed in centimeters.

Raman spectra have been recorded using a Dilor Labram micro-Raman spectrometer coupled to a microscope fitted with a 10X objective and equipped with a 1024 × 256 pixels CCD array. The excitation line was the 632.8 nm radiation from a HeNe laser (2 mW incident power on the sample).

Cyclic voltammetric experiments have been carried out at 20 ± 0.1 °C with a BAS 100 B electrochemical analyzer in a three-electrode cell. The working electrode is a 2 mm diameter platinum disk, polished to a mirror finish. The auxiliary electrode is a 2 mm diameter tungsten rod and a platinum wire is used as a quasi-reference electrode. The ferrocene/ferricinium (Fc/Fc^+) couple is used as an internal potential reference, according to the procedure recommended by IUPAC.[12] An ohmic drop compensation was applied when necessary.

Computational details

It will be shown below that a quantitative analysis of the absorption spectra requires the use of decomposition techniques. The decomposition method used is based on the nonlinear least-squares algorithm of Levenberg–Marquardt[13] and is performed with software developed in our laboratory. All decompositions of the absorption spectra have been performed on the energy scale, but the spectra are displayed on the wavelength scale. We have shown[14] that it is necessary to take into account the contributions of the solvent and of the quartz of the cell windows, because the spectra are recorded without any optical cell in the reference beam. The contribution of the quartz is weak but not negligible: the absorbance of quartz increases smoothly below 500 nm. It was taken into account as previously described:[14] it has been adjusted to the long-wavelength wing of a Gaussian band arbitrarily centered at 185 nm with a halfwidth of 35 000 cm^{-1}. These parameters are kept constant for all decompositions, but the maximum absorbance of this band is a variable parameter in the fit process because the thickness of the windows of the optical cells depends on the cell. The very fast increase of the absorbance of the solvent near 230 nm has been described by the sum of two Gaussian profiles, arbitrarily centered at 225 nm with halfwidths of 3500 and 8500 cm^{-1}. Those parameters have been determined for the pure solvent and they are kept constant in the decomposition of the absorption spectra of the SO_2–HMPA solutions.

The energy levels of SO_2 and S_2O_4 have been calculated using Wavefunction's Spartan molecular modeling tool[15] at the Hartree–Fock level with the 6-31G* basis set.

Results and discussion

Spectrophotometric study of SO_2–HMPA solutions

The UV/VIS absorption spectrum of an SO_2–HMPA solution displays only one absorption maximum, at about 270 nm (Fig. 1). This band is partly overlapped by the solvent absorption and it is necessary to decompose the spectra in order to get an accurate measurement of the absorbance of the solute. The spectra cannot be decomposed with a single Gaussian profile, which is the most usual lineshape for solution spectra.[16] The spectra cannot be satisfactorily decomposed either with a Lorentzian or a log-normal lineshape. Therefore, it is necessary to use a model with two Gaussian bands. During the decomposition procedure of each spectrum, the parameters of these two bands (wavelength at the absorbance maximum, linewidth and maximum absorbance) are allowed to vary. A given spectrum is completely described by the final set of these parameters. For each of the 15 spectra that were decomposed, the parameters of each band are similar: one absorption band is located at $\lambda_1 = 251.5 \pm 0.5$ nm, with a linewidth $\Delta\bar{\nu}_1 = 4200 \pm 200$ cm^{-1}; for the second absorption band, $\lambda_2 = 275.5 \pm 0.6$ nm and $\Delta\bar{\nu}_2 = 4500 \pm 100$ cm^{-1}.

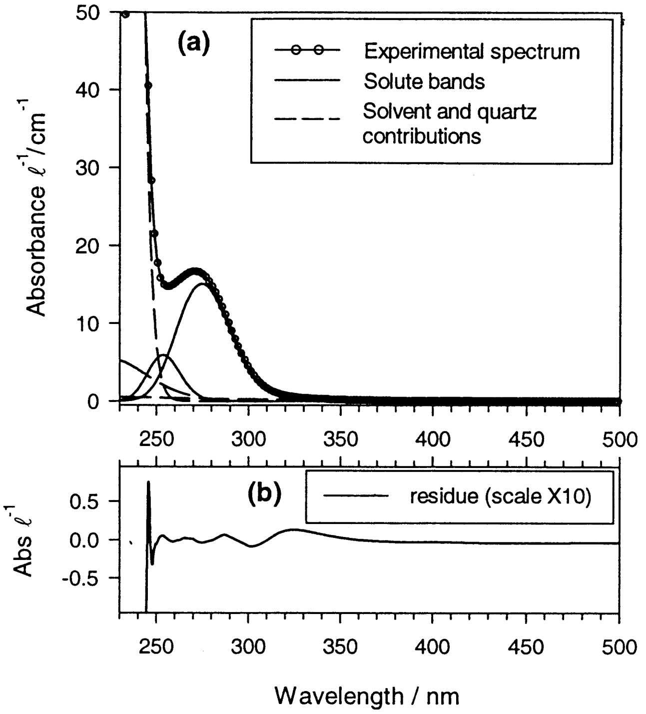

Fig. 1 UV/VIS absorption spectrum of a 10.25×10^{-3} mol dm^{-3} SO_2–HMPA solution. (*a*) Experimental spectrum and decomposition into five Gaussian bands, (*b*) residue of the adjustment. Note that the absorbance has been divided by the optical pathlength.

Fig. 1 shows one of the spectra after decomposition. With this model, the adjustment is very satisfactory, as indicated by the residue [Fig. 1(*b*): note that the residue is plotted on a ten-fold expanded scale]. The absorbance values given by the decomposition are plotted in Fig. 2 *versus* C_0 (the total SO_2 concentration). For the λ_1 band, the absorbance increases faster than C_0, while the variation of the absorbance of the λ_2 band with C_0 is linear. Consequently, these two bands cannot be assigned to the same species.

The existence of two absorption bands for SO_2 in solution was already mentioned by Eugène *et al.*,[17] in dimethylacetamide. After subtracting the solvent spectrum, two absorption maxima were observed, at 263 and 275 nm. No further interpretation was given by these authors. On the other hand, Booth *et al.*,[10] in their study of the complexation of SO_2 with olefins and aromatic compounds, observed a major absorption band at about 290 nm and, in some cases, a second band at a shorter wavelength. This second band is assigned to the SO_2–solvent charge-transfer complex. We can discuss this hypothesis in the case of SO_2–HMPA solutions; let us suppose the existence of a complex species X, which results from the complexation of SO_2 with HMPA:

$$SO_2 + \text{HMPA} \rightleftharpoons X \qquad (1)$$

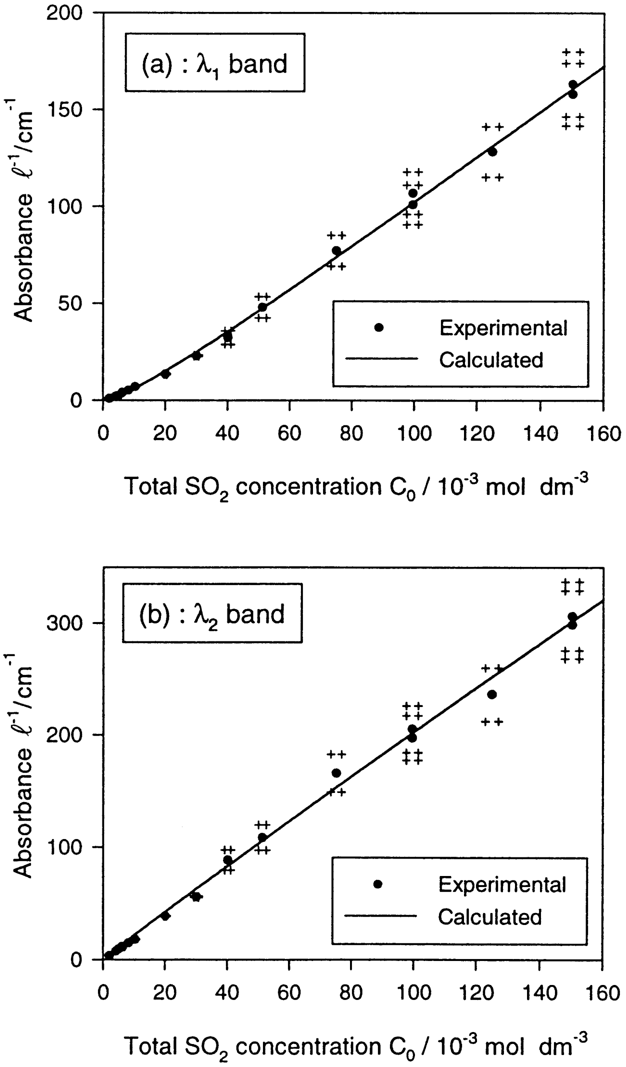

Fig. 2 Absorbance of the two bands, obtained after decomposition of the spectra, *versus* the total SO_2 concentration C_0, and calculated curve. Note that the absorbance has been divided by the optical pathlength. (*a*) First absorption band : $\lambda_1 = 251.5 \pm 0.5$ nm and $\Delta\bar{\nu} = 4200 \pm 200$ cm^{-1}, (*b*) second absorption band: $\lambda_2 = 275.5 \pm 0.6$ nm and $\Delta\bar{\nu} = 4500 \pm 100$ cm^{-1}.

The equilibrium constant of this reaction is given by:

$$K = \frac{[X]}{[SO_2]} \tag{2}$$

(HMPA being the solvent, its activity is taken equal to unity.) Moreover, the total amount of SO_2 is constant. Combining this with eqn. (2), we find that:

$$[X] = C_0 \frac{K}{1 + K} \tag{3}$$

[X] increases linearly with C_0 and so does its absorption band (within the range of dilute solutions). The absorbance of the λ_1 band increases faster than C_0. Consequently, this band cannot be assigned to a SO_2–HMPA complex with only one SO_2 unit, because its absorbance would increase linearly with C_0, as given by eqn. (3). The λ_1 band must then be assigned to a species containing more than one SO_2 unit, $(SO_2)_n$. In the cyclic voltammetric study of polythionite solutions,[6] the $S_2O_4^{-\cdot}$ species is clearly identified and it can be oxidized. This oxidation cannot lead directly to two SO_2 molecules because of the Franck–Condon principle, which states that the molecule configuration cannot change during the electron transfer. This suggests the existence of a sulfur dioxide dimer, S_2O_4, in SO_2–HMPA solutions, at least as a transitory species. Consequently, we propose that the λ_1 band is due to an associated species containing two SO_2 molecules. SO_2 and its dimer species, S_2O_4, are in equilibrium following the reaction:

$$S_2O_4 \rightleftharpoons 2SO_2 \tag{4}$$

$[S_2O_4]$ will increase faster than C_0, because the dimer species is favored (compared to SO_2) at high concentrations. The λ_1 band must then be assigned to the S_2O_4 species.

Let us now examine quantitatively the variations of the absorbance of the λ_1 and λ_2 bands *versus* C_0. The absorbances are given by the decomposition of the spectra (Fig. 2). The absorbance of the λ_1 band is given by:

$$\frac{A(\lambda_1)}{l} = \varepsilon(S_2O_4, \lambda_1)[S_2O_4] \tag{5}$$

$[S_2O_4]$ is expressed as a function of C_0 and K, the equilibrium constant for the dissociation of S_2O_4 into two SO_2 units (eqn. 4). This gives a theoretical expression for $A(\lambda_1)/l$ *versus* C_0 with two parameters: K and $\varepsilon(S_2O_4, \lambda_1)$. This equation was fitted to the experimental curve by using a nonlinear least-squares method.[13] The values obtained for the two parameters are: $K = (1.3 \pm 0.4) \times 10^{-2}$ mol dm^{-3} and $\varepsilon(S_2O_4, \lambda_1) = 2630 \pm 100$ dm^3 mol^{-1} cm^{-1}. The calculated curve for $A(\lambda_1)/l$ *versus* C_0 (using these values) is plotted in Fig. 2(*a*) (solid line).

Taking this value of K, the variation of $[SO_2]$ with C_0 can be calculated. The curve obtained is not linear: $[SO_2]$ increases less than C_0. The absorbance variation of the λ_2 band *versus* C_0 is linear, consequently this band cannot be assigned either to SO_2 only, or to S_2O_4 only. It must result from the superposition of two bands at very similar wavelengths, which cannot be discriminated in the decomposition of the spectra. We can then write:

$$\frac{A(\lambda_2)}{l} = \varepsilon(SO_2, \lambda_2)[SO_2] + \varepsilon(S_2O_4, \lambda_2)[S_2O_4] \tag{6}$$

Expressing $[SO_2]$ and $[S_2O_4]$ as functions of C_0 and K, we obtain the expression of $A(\lambda_2)/l$ *versus* C_0. The calculation process is the same as for the λ_1 band and gives: $\varepsilon(SO_2, \lambda_2) = 2410 \pm 440$ dm^3 mol^{-1} cm^{-1} and $\varepsilon(S_2O_4, \lambda_2) = 3840 \pm 230$ dm^3 mol^{-1} cm^{-1}. The calculated absorbance curve is displayed in Fig. 2(*b*) (solid line).

The value of K is less than unity, which indicates that the equilibrium favors the dimer species S_2O_4. This can be considered as a surprising result, because this species has never been identified in solution. However, the second absorption band (λ_1) cannot be seen unless the spectra are decomposed, which has never been done for SO_2 solutions before this work. Moreover, most of the previous studies were performed at low concentrations, for which SO_2 is still the major species (references given in ref. 1 and 6).

Previous studies have shown[10] that the molar extinction coefficient of SO_2 increases strongly when SO_2 is complexed. In these cases, the absorption band must in fact be assigned to the SO_2 unit inside the complex. Booth *et al.*[10] explained this enhancement of the absorption band by an increase of the 290 nm transition probability within the SO_2 molecule, due to the proximity of the molecule complexed with SO_2. Consequently, the ε values of SO_2 in solution depend strongly on the solvent:

nonpolar solvents (no complex formed):[9] $\varepsilon \approx 300$ dm^3 mol^{-1} cm^{-1}
oxygenated solvents:[9] $\varepsilon \approx 600$–800 dm^3 mol^{-1} cm^{-1}
aromatic compounds:[9] $\varepsilon > 1000$ dm^3 mol^{-1} cm^{-1}
amines:[7] ε is much higher (*e.g.* 5000 dm^3 mol^{-1} cm^{-1} for the SO_2–trimethylamine complex)

In HMPA, the values obtained are between 2500 and 4000 dm^3 mol^{-1} cm^{-1}. These high values indicate that both SO_2 and its dimer are complexed with the solvent. This was expected because HMPA {formula: $[(CH_3)_2N]_3PO$}, has several nucleophilic sites (N and O atoms)]. It is thus a strong Lewis base.

Spectrophotometric study of SO_2–TEAP–HMPA solutions

Addition of a supporting electrolyte is necessary for electrochemistry experiments. The dimerization equilibrium of SO_2 can be displaced because of the strong increase of the ionic strength due to the presence of a salt at high concentration. This led us to examine the influence of the addition of TEAP on the UV/VIS absorption spectra of SO_2–HMPA solutions, as TEAP is the supporting electrolyte used in our electrochemistry experiments (see below).

The procedure followed for SO_2–HMPA solutions is also used here: the absorption spectra are decomposed, then the absorbance of the λ_1 and λ_2 bands allows us to calculate the SO_2 and S_2O_4 concentrations in the solution, since the ε values are now known. Fig. 3 displays these concentrations *versus* C_0 for solutions without TEAP and for solutions containing 0.1 mol dm^{-3} TEAP. With the addition of TEAP, $[SO_2]$ increases while $[S_2O_4]$ decreases.

For the dissociation reaction of S_2O_4 (eqn. 4), the equilibrium constant is given by:[18,19]

$$K = \frac{(\gamma_{SO_2})^2}{\gamma_{S_2O_2}} \frac{([SO_2])^2}{[S_2O_4]} \tag{7}$$

where γ_i is the activity coefficient of the i species. SO_2 and S_2O_4 being rather similar species, it can be supposed that $\gamma_{SO_2} \approx \gamma_{S_2O_4} = \gamma$. At infinite dilution, the activity coefficients are equal to unity; this gives:

$$K = \gamma K_{\text{dil.}} \tag{8}$$

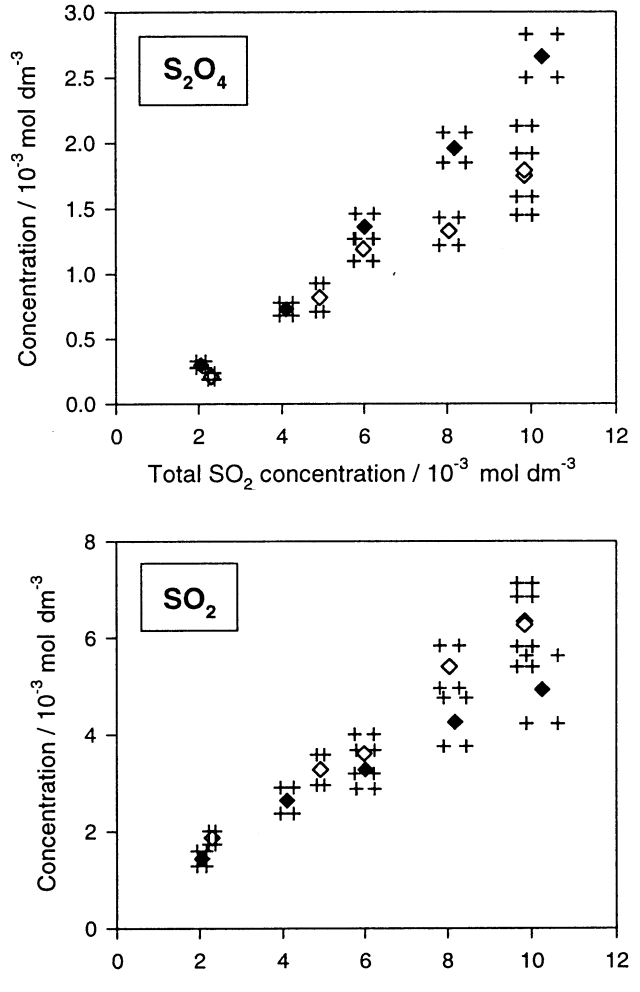

Fig. 3 SO_2 and S_2O_4 concentrations *versus* the total SO_2 concentration C_0. These values are obtained from the decomposition of the UV/VIS spectra. (◆) SO_2–HMPA solutions, (◇) SO_2–0.1 mol dm^{-3} TEAP–HMPA solutions.

SO_2 and S_2O_4 are neutral species, so Debye–Hückel theory cannot be used to calculate their activity coefficient.[19] The equation of Debye and McAulay[19] must be applied instead:

$$\ln(\gamma) = c\mu \tag{9}$$

where μ is the ionic strength and c depends on the temperature, the ionic radii of the ions present in the solution and the dielectric constants of the solvent and solute. c is positive if the dielectric constant of the solute is lower than that of the solvent and negative otherwise.[19] K can then be written as:

$$K = K_{\text{dil.}}\, e^{c\mu} \tag{10}$$

At room temperature, the dielectric constant of liquid SO_2 [4] is 13 and that of HMPA[11] is 29.6. Therefore, c is positive and K will increase when the ionic strength increases; in other words, the equilibrium will be shifted towards SO_2 when a salt is added. This fits well with the experimental observations: in the presence of TEAP, $[SO_2]$ increases while $[S_2O_4]$ decreases.

Raman study of SO_2–HMPA solutions

Table 1 presents the bands observed in the Raman spectra of SO_2–HMPA solutions at two concentrations, and those of the Raman bands of SO_2 in the gas phase.[4] For a dilute solution (0.05 mol dm^{-3}), we observed only the ν_1 vibration, nearly at the same frequency as in gaseous SO_2. The two other bands are too weak to be observed at this concentration. In a concentrated SO_2–HMPA solution (1 mol dm^{-3}), where S_2O_4 is the major species, the three Raman bands are observed, but their wavenumbers are shifted compared to those of gaseous SO_2.

Nxumalo and Ford[20] computed several possible structures for the sulfur dioxide dimer, as well as the vibrational frequencies for the three most probable structures. They found that these frequencies are shifted by about 5–10 cm^{-1} compared to those of SO_2. In the gas phase, S_2O_4 is a van der Waals complex where each SO_2 unit is slightly distorted, which results in a shift of the vibrational frequencies. Moreover, the bond between the two SO_2 units is too weak to give rise to a new vibrational band.

The shift of the Raman bands observed in concentrated SO_2–HMPA solutions relative to the frequencies observed for SO_2 in the gas phase are of the same order of magnitude as those calculated for S_2O_4;[20] this supports the presence of S_2O_4 in solution.

Electrochemical study

Typical cyclic voltammograms recorded on a Pt electrode for SO_2–HMPA solutions are displayed in Fig. 4. Two reduction peaks can be seen at very close potentials. This is also observed for a glassy carbon electrode in HMPA, and Kim and Park[21] observed a similar splitting in DMSO, but without giving any interpretation. The cyclic voltammetric study of polythionite solutions, $Li(SO_2)_n$–HMPA, suggested the existence of two redox couples:[6] $SO_2/SO_2^{-\cdot}$ and

Table 1 Position of Raman bands (cm^{-1}) of SO_2 in the gas phase and in SO_2–HMPA solutions

Vibration assignment	Pure SO_2 (gas phase)[a]	SO_2–HMPA $C_0 = 0.05$ mol dm^{-3}	SO_2–HMPA $C_0 = 1$ mol dm^{-3}
ν_2 (bending)	524	n.o.	530
ν_1 (sym. str.)	1145	1147	1142
ν_3 (asym. str.)	1334	n.o.	1320

[a] Ref. 4. n.o.: not observed (too weak).

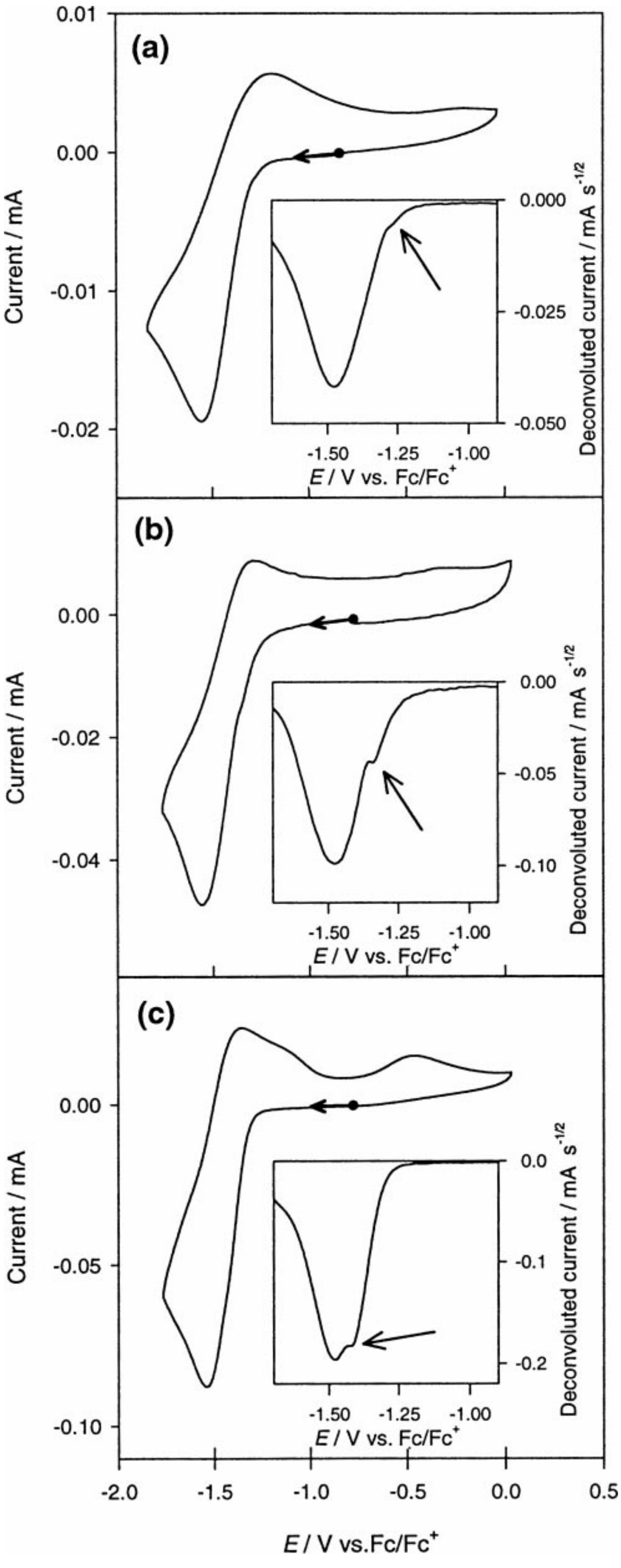

Fig. 4 Cyclic voltammograms of SO_2–HMPA solutions. The main curve is the experimental voltammogram; the insert displays the first vertex of the deconvoluted voltammogram. The initial potential is the equilibrium potential of the solution. Working electrode: Pt, area 3.14 mm^2, scan rate 1 V s^{-1}. $C_0 = (a)$ 2.3, (b) 4.92, (c) 9.84 × 10^{-3} mol dm^{-3}.

$S_2O_4/S_2O_4^{-\bullet}$. We have shown previously[6] that the first reduction peak (the so-called prewave), which is the smaller one, is the reduction of S_2O_4 and that the second peak is the reduction of SO_2. The interpretation of some of the anodic peaks has been discussed elsewhere[6] and work is in progress in order to interpret the cyclic voltammograms over the whole potential range.

A further indication for the attribution of the two reduction peaks can be deduced from the respective values of the electron affinities of SO_2 and S_2O_4. The geometry of SO_2 and S_2O_4 has been previously studied.[20,22] Using these results, we calculated the energy levels for each possible geometry. The reduction potential of a species is related to its electron affinity, that is, the LUMO energy.[23] The electron affinity of S_2O_4 was calculated for each of the most probable structures. In each case, it was found to be 60 to 70 meV higher than that of SO_2; this means that the reduction potential of S_2O_4 should be slightly higher than that of SO_2. On the voltammograms, the prewave is observed at a potential about 150 mV higher (*i.e.*, more positive) than that of the main peak, which is the reduction of SO_2.

The cathodic part (first vertex of the potential ramp) of the voltammograms was then deconvoluted, (Fig. 4, insert) in order to get a better resolution of these two peaks. The deconvolution[24] is another representation of the experimental results; it is numerically deduced from the current-potential data. It offers several advantages: the deconvoluted peaks observed for reversible electrode processes are symmetrical and sharp whereas conventional current-potential peaks are asymmetrical and rather broad. This representation provides then a better resolution than standard voltammetry.

The height of the two peaks, that is, the intensity of the deconvoluted current, is correlated with the amount of SO_2 and S_2O_4 present in the solution at equilibrium, which is given by the spectrophotometric study. When the total SO_2 concentration increases, the S_2O_4 concentration increases relative to the SO_2 concentration, and the height of the first reduction peak increases relative to the second one. The voltammograms were recorded at a relatively fast scan rate (1 V s^{-1}) in order to minimize kinetic effects during the cyclic voltammetry experiment. The dissociation equilibrium of S_2O_4 is a homogeneous chemical reaction (eqn. 4) coupled to the charge transfer, and the kinetic effect of this reaction is not negligible at slow scan rates. In these conditions, the prewave will be more intense than expected from the value of the concentration at equilibrium, because the S_2O_4 consumed will be replaced through this reaction. Only at a very fast scan rate would this effect disappear.

This clear relationship between the concentration of the species at equilibrium and the peak currents measured in cyclic voltammetry allows one to confirm both the existence of the dimer species S_2O_4 and the attribution of the prewave to its reduction. These two results, along with the determination of the value of the equilibrium constant, will be very helpful for the understanding of the chemical reactions coupled to the SO_2 reduction, and for interpretation of the whole voltammograms stated above.

Conclusions

The spectrophotometric study of SO_2–HMPA solutions, and the decomposition of spectra, show that SO_2 is in equilibrium with a dimer species S_2O_4. The study of the absorbance of the two bands *versus* the total SO_2 concentration allowed us to determine the equilibrium constant of the dissociation of S_2O_4 (into two SO_2 units). The influence of the addition of a supporting electrolyte has been examined: it shifts the equilibrium towards SO_2, as expected for equilibria involving neutral species.

The Raman spectroscopic study also indicates the presence of S_2O_4 in SO_2–HMPA solutions: the vibration frequencies are shifted relative to those of SO_2, as expected from previous studies.

These results are correlated with the electrochemical study: the S_2O_4 reduction is observed as a prewave on the cyclic voltammograms, about 150 mV before that of SO_2. This could also be deduced from the respective electron affinities of these two species, which have been calculated here. Moreover, the intensity of this prewave is related to the concentration of S_2O_4 in the solution. This confirms both the existence of this species and the attribution of the prewave to its reduction.

Acknowledgements

The authors are grateful to Dr. M. De Backer for his help in calculating the electron affinities, and to Dr. F.-X. Sauvage for a critical reading of the manuscript. The help of Dr. M.-C. Dhamelincourt for the recording of the Raman spectra is acknowledged. One of the authors (EP) wishes to thank the 'Ministère de l'Education Nationale et de l'Enseignement Supérieur et de la Recherche' for granting her a doctoral scholarship.

References

1 E. Potteau, J.-P. Lelieur and E. Levillain, *New J. Chem.*, 1997, **21**, 521.
2 D. Devèze and P. Rumpf, *C. R. Séances Acad. Sci., Paris, Série C.*, 1968, **266**, 1001.
3 A. Taleb-Bendiab, K. W. Hillig II and R. L. Kuczkowski, *J. Chem. Phys.*, 1991, **94**, 6956.
4 D. F. Burow, in *The Chemistry of Non-aqueous Solvents*, ed. J. J. Lagowski. Academic Press, New York, 1966, vol. 3, p. 137.
5 L. M. Nxumalo and T. A. Ford, *J. Mol. Struct.*, 1995, **347**, 495.
6 E. Potteau, E. Levillain and J.-P. Lelieur, *J. Electroanal. Chem.*, 1997, **436**, 271.
7 J. Grundnes and S. D. Christian, *J. Am. Chem. Soc.*, 1968, **90**, 2239.
8 M. W. Wong and K. B. Wiberg, *J. Am. Chem. Soc.*, 1992, **114**, 7527.
9 L. J. Andrews and R. M. Keefer, *J. Am. Chem. Soc.*, 1951, **73**, 4169.
10 D. Booth, F. S. Dainton and K. J. Ivin, *Trans. Faraday Soc.*, 1959, **55**, 1293.
11 C. K. Mann, in *Electroanalytical Chemistry*, ed. A. J. Bard. Dekker, New York, 1969, vol. 3, p. 92.
12 G. Gritzner and J. Kuta, *Pure Appl. Chem.*, 1984, **56**, 461.
13 W. H. Press, B. P. Flamery, S. A. Teukowski and W. T. Vetterling, *Numerical Recipes*, Cambridge University Press, Cambridge, 1984.
14 P. Leghié, E. Levillain, J.-P. Lelieur and A. Lorriaux, *New. J. Chem.*, 1996, **20**, 1121.
15 *Spartan version 5.0*, Wavefunction, Inc., Irvine, CA USA, 1997.
16 B. E. Barker and M. F. Fox, *Chem. Soc. Rev.*, 1980, **9**, 143.
17 F. Eugène, B. Langlois and E. Laurent, *New. J. Chem.*, 1993, **17**, 815.
18 P. Souchay, *Thermodynamique Chimique*, Masson, Paris, 1967, ch. 15.
19 H. S. Harned and B B Owen, *The Physical Chemistry of Electrolytic Solutions*, Reinhold, New York, 1949, ch. 3 and 12.
20 L. M. Nxumalo and T. A. Ford, *Spectrochim. Acta, Part A*, 1995, **51**, 1847.
21 B.-S. Kim and S.-M. Park, *J. Electroanal. Chem.*, 1995, **142**, 26.
22 R. G. A. Bone, C. R. Le Sueur, R. D. Amos and A. J. Stone, *J. Chem. Phys.*, 1992, **96**, 8390
23 A. J. Bard and L. R. Faulkner, *Electrochemical Methods, Fundamentals and Applications*, Wiley, Chichester, 1980.
24 J.-S. Yu and Z.-X. Zhang, *J. Electroanal. Chem.*, 1996, **403**, 1 and references cited therein.

Paper 8/03637C